HKD
1926

Poetics of Interplay and Interferences of Potentiodynamic Sweeps and Peaks in Electrocatalysis for Oxygen Electrode Reactions

Jelena M. Jaksic,[1] Caslav M. Lacnjevac,[2] Milan M. Jaksic,[1,2,*]

[1] Institute of Chemical Engineering Science, ICEHT/FORTH, Patras, Greece

[2] Faculty of Agriculture, University of Belgrade, Belgrade, Serbia

[*] Corresponding author's e-mail address: milan@iceht.forth.gr

─── THIS PAPER IS DEDICATED TO PROF. MIRJANA METIKOŠ-HUKOVIĆ ON THE OCCASION OF HER BIRTHDAY ───

Abstract: Strong irreversible adsorptive monolayer growth of the surface (Pt=O→1), out of the reversible primary (Pt−OH→0) oxides, imposes typical highly pronounced *reaction polarization*, and that way prevents, at least partially, the reversible electrocatalytic properties and behavior of even all plain and non-interactive supported noble metals (Pt, Pt/C) for oxygen electrode reactions, within closed loop of potentiodynamic spectra between hydrogen and oxygen evolving limits. Substantially quite another type of assembly afford nanostructured hyper-d-electronic-metals (Pt,Au,Ru), interactive grafted upon hypo-d-(f)-oxide supports, in particular of mixed and higher alter-valence values (W,Mo,Ta,Nb), well and for longer known in heterogeneous catalysis as SMSI (Strong Metal-Support Interaction, the ones of strongest in the entire chemistry). The most promising being Magneli phases (MPs, $Ti_nO_{(2n−1)}$, or Ti_4O_7 in average, and as the optimum in catalytic activity), which arise after simple thermal recrystallization (pure entropy change contribution) yield effect, out of anatase and/or rutile titania (TiO_2). The main accompanying achievements of substantial significance then have been: (i) Prevailing percentage in spontaneous adsorptive dissociation of molecular water upon hypo-d-(f)-oxide surfaces, or the corresponding latent storage and spillover of the yielding primary oxides (Pt−OH); (ii) Extra high stability MPs, (Plate type electrodes of MPs are straightforward employed in industrial chlorate cell production, and/or Li-batteries); (iii) Spontaneously adsorptive dissociated water molecules (or, hydroxide ions), then undergo membrane type ionic transfer all along hypo-d-(f)-oxide supports, until approaching catalytic metal surface, when the latter takes the prevailing amount of electron charge, and that way creates the primary oxide dipole species (Pt−OH); (iv) these undergo spillover by repulsion upon metallic, hypo-d-(f)-oxide and even over the suboxide MPs surfaces; (v) while the Magneli phases themselves feature a rather high n-type electron conductivity (up to and even above 1,000 S/cm). The wetness impact factor and effect have been introduced as the lowest threshold level associated with the Pt−OH (Au−OH), bellow which there is no (electro)catalytic oxidation reaction taking place, such as the CO tolerance. The overall result of the present study has then been the development and achievement of the reversible electrocatalysts for the oxygen electrode reactions (ORR, OER), primarily for L&MT PEMFCs.

Keywords: spillover, primary oxide (Pt−OH), surface oxides (Pt=O), Magneli phases (MPs), latent Pt−OH storage, reaction polarization, spontaneous adsorptive dissociation, polarization barrier, CO tolerance.

INTRODUCTION

POTENTIODYNAMIC sweeps and/or cyclic voltammetry spectra appeared in the previous century remarkably postponed relative to the whole field of electrochemical science. Meanwhile, it was still preceding to the entire development of its main area – Electrocatalysis, but in any case the effect of the adsorptive intermediate oxides for heterogeneous electrode reactions was unknown. Thus, the initial and standard type voltammograms imply the potential sweep rate as the main first interactive variable to scan all peaks and all intermediates interplaying and interfering redox states, the range of their appearance and/or missing, which in stationary polarization measurements usually mutually interdependently overlap or undergo superposition into the apparent steady-states or Tafel line plots. In fact and in the effect, potential sweep rate substantially defines and reflects the main electrocatalytic parameter (mV/s). This is the reason that and why kinetic measurements imply now primarily low
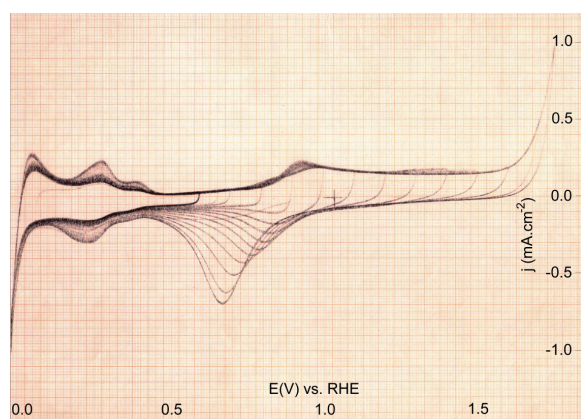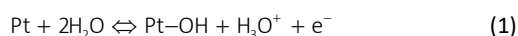
Figure 1. Cyclic voltammograms of polycrystalline Pt scanned in 0.1 M NaOH at sweep rate 100 mV·s⁻¹(Reprinted with permission from Ref. [7]. Copyright (2014) American Chemical Society).

value sweep rates for stationary and appear reliable to assessing *quasi* steady-state polarizations and construct typical Tafel plots in kinetic evaluations, and distinguish the reversible from irreversible range and behavior. In aqueous mineral acid and alkaline solutions, H-adatoms along with various surface adhering oxides (Pt–OH, Pt=O), and their interplay within characteristic reversible and irreversible peak potential values and properties, enable us to select and define best and most reliable electrocatalytic species for *a priori* defined catalytic electrode processes. Such state of actual potentiodynamic knowledge and experience logically impose the question are there any abilities to extend the reversible into and even all over the corresponding potential range of its irreversibility, and effectively provide and continuously (endlessly) maintain the necessary electrocatalytic activity for electrode processes, such as the cathodic ORR and OER? Such an aim and target would be the subject matter and challenge purpose of the present study, while thermodynamically reversible in electrocatalytic activity and performances resulting from the relevant interfering potentiodynamic knowledge and congenial experience. For composite solar photo voltaic systems, as the main sustainable world energy strategic approach, thermodynamic reversibility for the ORR is the core target and basic implied assumption (30 mV/dec, not more than 60 mV/d).
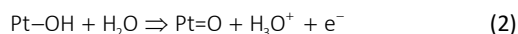
Interference of Potentiodynamic Sweeps and Peaks, Predicting and Revealing Electrocalytic Activity

The initial potentiodynamic scans in alkaline media (Figure 1) have been primarily focused on noble (Pt,Au) metals, while the reversible primary (Pt–OH, Au–OH) and polarizable surface (Pt=O, Au=O) oxides, along with H-adatoms (Pt–H,

Au–H), represent interactive species defining the broad overall plain (Pt,Au) and/or non-interactive supported (Pt/C, Au/C) electrode behavior and properties.[1–3] The latter means and includes all redox occurrences in between of cathodic hydrogen and anodic oxygen evolving limits, revealed by corresponding peaks within cyclic voltammetry spectra dependent only on the potential sweep rate. Meanwhile, these adsorptive hydrogen and oxygen species and their decisive electrocatalytic and/or polarizable effects belong to newer developments in the electrochemical science,[1–3] and while missing, the whole kinetic and catalytic knowledge and understanding for longer were unclear and obscure. In such a respect potentiodynamic spectra (Figure 1), usually reveal within a narrow potential range the highly reversible peaks of primary oxide (Pt–OH) adsorptive growth, along with self-catalytic stepwise molecular water oxidation, and its backwards desorptive removal,[1–3]

$$Pt + 2H_2O \Leftrightarrow Pt-OH + H_3O^+ + e^- \qquad (1)$$

as a typical double layer (DL) charging and discharging pseudo-capacitance.[4–8] Meanwhile, the former soon later irreversibly disproportionates (Pt–OH→0), into the strongly polarizable, more adsorptive and more stable surface oxide (Pt=O→1) monolayer,[1–3]

$$Pt-OH + H_2O \Rightarrow Pt=O + H_3O^+ + e^- \qquad (2)$$

with the corresponding pronounced irreversible desorption peak all along the equivalent reversal cathodic potential scan direction (Figure 1). The latter, in the entire absence of the Pt–OH, thereby imposes such a critical and typical, very pronounced ***reaction polarization range*** (Figure 1), (Pt–OH→0, Pt=O→1), the one of very exagereted in the whole electrochemistry all along until oxygen evolving potential limits, and in both scan directions, back and forth.[4–8] Such highly reversible (Equation 1), relative to the subsequent strongly irreversible, and substantially polarizable (Equation 2) transient, has been decisive as concerns the overall electrocatalytic properties and behavior of both Pt and Au, and more or less so for all other plain noble and even many non-noble transition metal electrodes for the oxygen electrode reactions (ORR and OER). Meanwhile, while dealing with simple electrode reactions of cathodic hydrogen evolution (and/or its anodic oxidation), and anodic oxygen evolution (and/or its cathodic reduction), researchers formerly, in the absence of cyclic voltammetry, omitted to reveal that the interrelation between the primary (Pt–OH) and surface (Pt=O) oxide defines the main polarization properties of plain (Pt) and non-interactive supported metal (Pt/C) catalyst. In other words, within the entire voltammogram, regardless the highest noble metal features, Pt(Au) behaves partly reversible, and along longer potential sweep, highly polarrizable. Thus, there is no single plain
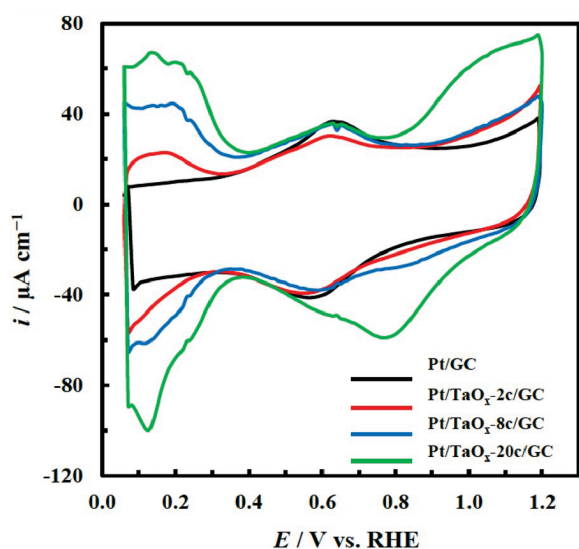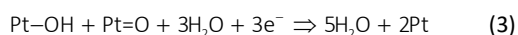
Figure 2. Cyclic voltammograms scanned at the Pt/GC and Pt/TaOx/GC catalytic electrodes with 2c, 8c, and 20c (cycles) in Ar-saturated 0.5 M H_2SO_4 solution at scan rate of 50 mV s^{-1}, revealing the effect of proportional increasing of interactive Pt supporting Ta_2O_5 deposit on the Pt-OH spillover effect and latent storage growth for the ORR (courtesy of T. Ohsaka[11]).

noble metal in the Periodic Table, regardless its precious features, to behave reversible for hydrogen and oxygen electrode reactions within the entire potential range between their evolving limits, back and forth.[6,7]

Since the equimolar ratio of the primary and surface oxide concentrations defines the optimal interfering self-catalytic spillover reaction step in cathodic oxygen reduction (ORR),[9] or as the overall electrode reaction,

$$Pt-OH + Pt=O + 3H_2O + 3e^- \Rightarrow 5H_2O + 2Pt \qquad (3)$$

and in particular along the reversible (low slope, 30 mV/dec, or even lower) parts of Tafel line plots, the irreversible disproportionation itself (Equation 2), imposes an extremely high **reaction polarization barrier** (Pt–OH→0, Pt=O→1) that amounts for even more than 600 mV s and then, in absence of the Pt–OH spillover reactant, makes plain Pt (and Au) and non-interactive supported both (Pt/C or Au/C) platinum and gold irreversible for the oxygen electrode reactions within the broader potential range, back and forth (Figure 1). The thermodynamic definition of irreversibility within closed loop of reaction circles, then would state that plain Pt(Au) by no means can feature the reversibility and/or (electro)catalytic activity all along the potential range in aqueous media. In other words, plain and non-interactive (Pt/C and/or Au/C) supported Pt(Au) electrodes themselves by no means can behave electrocatalytic features of the reversible oxygen
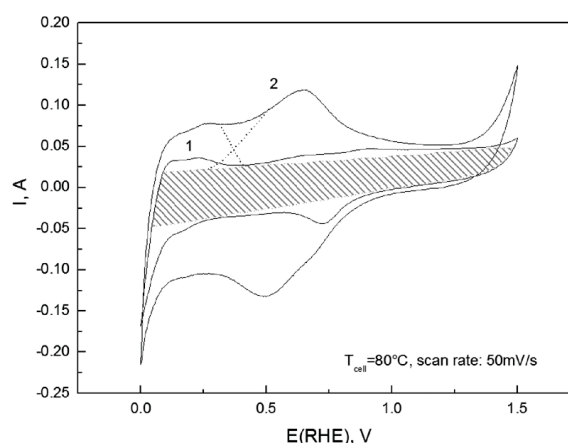

Figure 3. Cyclic voltammograms of mixed valence hypo-d-oxides supported nanostructured Pt electrode (Pt/TiO$_2$, WO$_3$/C), scanned in He stream, ones at negligible moisture content (curve 1) and at 80 °C water vapor saturation (curve 2) (Reprinted with permission from Ref. [7]. Copyright (2014) American Chemical Society).

electrode (ROE) all along the potential axis between hydrogen and oxygen evolving limits, back and forth. The strongly adsorptive and thence highly polarizable Pt=O (Au=O), deprived from any local and/or external Pt−OH (Au−OH) surface source and supply, then defines one of the most pronounced issues of the '*reaction polarization*' in the entire electrochemical science: No Pt−OH, means that there is no reversible reaction (Equation 3). Quite another story arises when nanostructured Pt(Au) electrocatalyst is interactive selective grafting bonded on various, in particular mixed valence hypo-d-(f)-oxide supports.[4–8] Meanwhile, although interactive SMSI-(Strong Metal-Support Interaction[10]) hypo-d-d-oxide supported catalysts (Pt) have already been broadly and for longer successfully employed in heterogeneous catalysis, electrochemists still hesitated to employ them, mostly because of erroneous expectancy for imposing to increasing IR-drop, and eventual chemical instability. In such a constellation, majority of transition (or d-metals), but primarily hyper-d-electronic elements plot their cyclic voltammograms in aqueous media as asymmetric spectra of well separated reversible from irreversible or polarizable parts: the former extends from the potential range of cathodic hydrogen evolution (or its anodic oxidation), till the peak of primary oxide deposition (or removal), and the latter initiating from the disproportionation of primary into polarizable surface oxides, back and forth scans all along the entire sweeps between the former and the gas oxygen evolving limits. The causes and reasons for such overall specific or general potentiodynamic behavior have just been displayed for the ones of most important issues (Pt(Au)).

The present analysis is best reflected and proved by comparison of Figures 1–3, once when missing Pt–OH spillover (Pt–OH → 0, Pt=O → 1), then when there proceeds simple effusion of self-generated Pt–OH,[11] or finally, when enriched latent storage spillover enables enormous primary oxide adsorptive deposition and reverse desorption, (Pt–OH → 1, Pt=O → 0). In other words, when the interactive hypo-d-(f)-oxide supports impose and continuously provide the latent storage and spillover supply of primary oxide, then potentiodynamic spectra keep the same general shape, but the reversible currents take dramatically higher values. In such a respect, since potentiodynamic spectra reveal by matching peaks and their specific type and nature, all subtle redox occurrences in between of hydrogen and oxygen evolving limits, as the final and main products of electrode reactions, cyclic voltammetry represents the mine electrochemical analytical tool and system for characterization of all electrode events and their properties, in particular in electrocatalysis.

Spontaneous Adsorptive Dissociation of Water Molecules, and Resulting Primary Oxide Latent Storage and Spillover

The first decisive step towards spontaneous latent storage and rather fast spillover widespreading phenomena of the Pt–OH is the consequence of a strong first principle thermodynamic confirmed evidence (Density Functional Calculations, DFC) by Vittadini *et al.*,[12] that water molecules undergo prevailing spontaneous dissociative adsorption on anatase (101), even rutile titania, and more so on the higher altervalent oxides[13] of tungsten, molybdenum, tantalum, niobium and/or cerium, *etc.*, (Figure 4), as the general oxophilicity properties of hypo-d-metal oxides. In addition, the simultaneous first-principles molecular-dynamic showed the existence of a mechanism for thermodynamically favored spontaneous dissociation of water molecules even at low coverage of oxygen vacancies of the anatase (101) surface,[13] and consequently even more so at the Magneli phases (MPs),[14,15] as substantially suboxide structure significant both as highly electronic conductive (up to and even more than 1,000 S/cm), perfect membrane type surface and bulk network transferring hydroxide specie, and ideal interactive hypo-d-oxide type catalyst support.[16,17] In fact, this is the status of reversible open circuit spontaneous dissociative adsorption of water molecules at the equilibrium state, something like capillary phenomena in adsorption after some critical coverage extents. Meanwhile, in the presence of the nano-sized and interactive supported metallic part of the catalyst, and continuous enough moisture supply, directional electric field (or, electrode polarization), further disturbs such an established equilibrium and dynamically
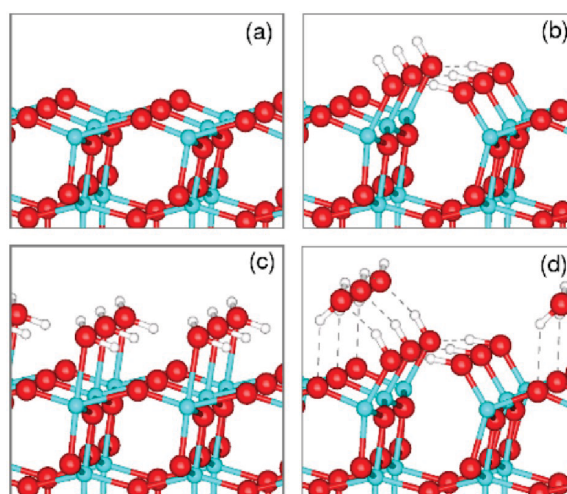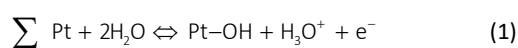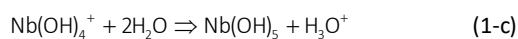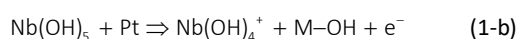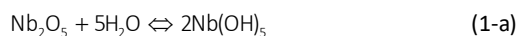

Figure 4. The perspective views of DFT-optimized atomic structures for: (a) the clean anatase (ADM) ad-molecule model of unreconstructed (001) surface; (b) the dissociated state of water (0.5 monolayer) on (001); (c) the relaxed geometries of molecular state of adsorbed water (1.0 monolayer of hydroxylated anatase) on (001); and (d) the mixed state of water on (001) with a half-dissociated coverage of adsorbed monolayer water molecules (courtesy of A. Vittadini, *cf.* Ref. [12]).

imposes further continuous forced dissociation of water molecules, and as the consequence, their membrane transport properties (Livage *et al.*[18–20]). Furthermore, majority of hypo-d-(f)-oxides and in particular of higher altervalent numbers, and consequently increased oxophilicity properties, feature prevailingly high percentage of spontaneous dissociative water molecules adsorption,[12,13] (Equation (1-a)), and thence, the enhanced surface membrane type of hydroxyl ions migration mass transfer,[18–20] (Equation (1-b) and (1-c)), the latter being, as the XPS measurements show,[6–8] even some sort of the common interfering effect, too,

$$Nb_2O_5 + 5H_2O \Leftrightarrow 2Nb(OH)_5 \qquad (1\text{-}a)$$

$$Nb(OH)_5 + Pt \Rightarrow Nb(OH)_4^+ + M\text{–}OH + e^- \qquad (1\text{-}b)$$

$$Nb(OH)_4^+ + 2H_2O \Rightarrow Nb(OH)_5 + H_3O^+ \qquad (1\text{-}c)$$

$$\sum \; Pt + 2H_2O \Leftrightarrow Pt\text{–}OH + H_3O^+ + e^- \qquad (1)$$

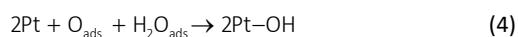ending up with the prevailing electron transfer to the interactive supported metallicatalyst, so that the Pt–OH(Au–OH) behaves as a pronounced dipole species,[21] and thus, exhibits the strong spillover surface repulsion, transfer and distribution, so that summation (∑) yields

Equation (1), definitely resulting with the pronounced latent storage and the Pt–OH dipole spillover features (Scheme 1).
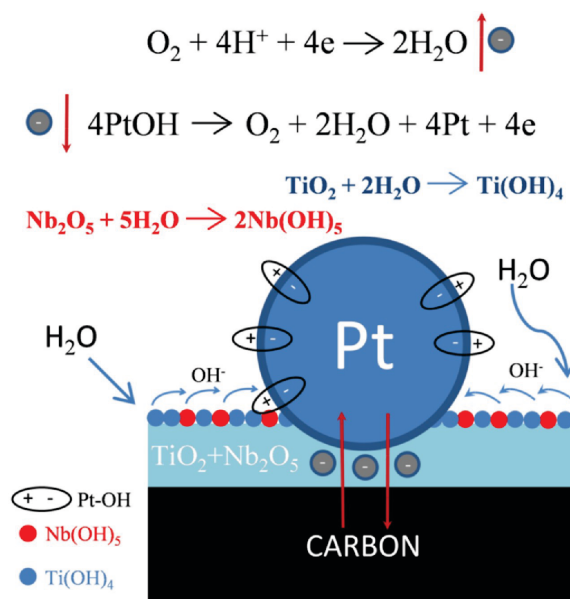
Such an individual, and in particular mixed valence oxide network, of polyvalent (high altervalent numbers) hypo-d-elements, when in hydrous state, distinctly behaves as an ion exchange membrane even for their own surface hydroxide migration. In fact, gels (aero and xerogels) are biphasic systems in which solvent molecules are trapped inside an oxide network, and such a material can be considered as a water-oxide membrane composite.[18–20] At the same time, the highly pronounced reversible potentiodynamic peaks testify for the extremely fast and independent overall spillover reaction (Equation 1), in both directions,[1–3] primarily used for DL charging and discharging pseudo-capacitance,[4–8] and being always available for heterogeneous electrode reactions, dynamically spontaneous dissociative water molecule adsorption always being more pronounced for less distributed (Magneli phases and similar) suboxide structures, then, for example, more rich anatase TiO_2 oxide itself.

Electrocatalytic Spillover Phenomena

The first spillover phenomenon in heterogeneous catalysis was observed and defined by Boudart[22,23] for the interactive supported bronze type (Pt/WO_3) catalyst, initially at high temperature (above 400 °C) for pure solid oxide system. Meanwhile, after the spontaneous adsorptive dissociation of water molecules on hypo-d-oxide supports of Pt,[22,23] the fast interactive effusion of H-adatoms over its hydrated ($W(OH)_6$) surface becomes dramatically sped up even at ambient conditions in the ultimate presence of condensed at least monolayer aqueous precipitate, and *vice versa*, establishing capillary phenomena of speeding up spillover of the main catalytic reaction intermediates (Pt–OH, Au–OH). Such a striking sharp wetness impact upon the overall spillover phenomena associated with hydrated hypo-d-oxides in aqueous media, implies Ertel[24] *auto-catalytic molecular water effect,* too, which states that the catalytic reaction of hydrogen oxidation upon Pt surface, even at deep low temperatures (140 K), proceeds with remarkable amounts of the Pt–OH, as the decisive and accumulated intermediate, including the unavoidable self-catalytic step with otherwise spontaneously adsorbed water molecules (equivalent to Equation 1),[12,13,24]

$$2Pt + O_{ads} + H_2O_{ads} \rightarrow 2Pt–OH \qquad (4)$$

In fact, Ertel has pointed out the substantial overall significance of water molecules in heterogeneous catalysis for oxidation processes that in general proceed over the Pt–OH generation and spillover, and substantially implies both the spontaneous adsorptive dissociation of water on

Scheme 1. Visual presentation of novel spillover latent storage Pt-OH type interactive supported electrocatalyst for oxygen electrode reactions, exampled for Pt/Nb_2O_5, $TiO_2/Nb(OH)_5$,$Ti(OH)_4$ issue (Reprinted with permission from Ref. [7]. Copyright (2014) American Chemical Society).

hypo-d-oxide supports,[12,13] and subsequent fundamental peak relations (Equation 1) on the same wet way in (electro)catalysis.
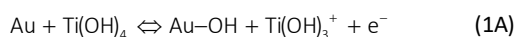
This is significant both for the evidence of the extremely fast spillover widespreading and thereby resulting with imposed the reversible hydrated substrate reduction. The latter finally leads to the corresponding form of electrocatalytically active bronze ($Pt/H_{0.35}WO_3$) for cathodic processes, in which non-stoichiometric incorporated hydrogen obeys the same free reactive properties like adsorptive (Pt–H), and is the main source for the electrode or heterogeneous catalytic reactions. In other words, the point is that spontaneous dissociative adsorption of water molecules[12,13] imposes much smaller activation energy for transformation of the resulting hydrated $W(OH)_6$, into corresponding bronze state, and *vice versa*, and occurs even at ambient temperature, then behaving remarkably different than the initial solid oxide WO_3. Thence, such a wet adsorptive dissociate species (H_2O-molecular) and capillary adhering hypo-d-oxide support dramatically facilitates the overall spillover effect under pronounced wet status (the activation energies thence being in the ratio of 2.2, one with another). The alterpolar interchanges between the bronze type electrocatalyst and its hydrated state are correspondingly approved occurring instantaneously and reversibly fast, because of the substantially facilitated Boudart[22,23] spillover effect, and behave as a thermodynamic

equilibrium (Pt/H$_{0.35}$WO$_3$ $\Leftrightarrow$ Pt/W(OH)$_6$). In other words, such state of the art enables to perform and even speedup (electro)catalytic processes from very high temperature down at ambient conditions, simply by the impact of adsorptive wetness effect.[6–8,12,13,24]

The Impact Self-Catalytic Molecular Water or Overall Wetness Effect

In such a respect, it is certainly worth mind keeping the self- or auto-catalytic Ertel[24] effect of water molecules for the Pt–OH growth that mostly occurs in all heterogeneous (electro)catalytic oxidation processes, Equation 4, particularly when these water molecules appear as dipoles polarized within double layers (Equation 1).[21] Haruta[25,26] in the same sense has pointed out the lowest impact threshold moisture content below which there is no CO oxidation upon otherwise ideal interactive supported catalysts (nanostructured Au/TiO$_2$).[27–29] In fact, there establishes an entirely thermodynamic equilibrium (Pt/H$_x$Nb$_2$O$_5$ $\Leftrightarrow$ Pt/Nb(OH)$_5$), which enables the instant-aneous reversible alterpolar interchanges and therefrom the substantiation of superior revertible cells altering between PEMFCs and WE (Water Electrolysis), otherwise being of substantial significance for the hydrogen energy balance, and performances. In other words, no spillover of primary oxides (Pt–OH, Au–OH), substantially means that there are no reversible alterpolar changes and no advanced revertible PEMFCs!

The most fascinating results in heterogeneous catalysis obtained Haruta,[25–27] (*wetness impact*) long ago with nanostructured gold interactive supported upon anatase titania (Au/TiO$_2$). The same nano-size Au clusters, once plain, then on the indifferent ZnO carrier, and upon hypo-hyper-d-d-interelectronic titania supporting bonded, so that these mutually differ for several orders of magnitude in catalytic activity for the highly efficient reaction (trace amounts removal level for human protection) with CO at the extremely low impact water threshold levels.[25–29] The same catalyst metal (Au) differed only in the interactive hypo-d-oxide anatase titania (101) support presence and/or absence, or instead, the indifferent ZnO was compared as the non-interactive oxide catalyst support, while the catalytic activity has been distinctly, exponentially different and broadly proved. For the catalytic science it was *a priori* clear that some superior reaction occurs initiated at and provided by the exposed titania surface.[4–8] In other words, the latter is in advance predestined ready and highly susceptible for spontaneous dissociative adsorption of water molecules (TiO$_2$ + 8H$_2$O $\Rightarrow$ Ti(OH)$_4$ + 4H$_3$O$^+$), otherwise already being revealed as the subject of latent storage and the Au–OH spillover,[5–8,12,13] decisive for both heterogeneous catalytic oxidation and reduction reactions,

$$Au + Ti(OH)_4 \Leftrightarrow Au\text{–}OH + Ti(OH)_3^+ + e^- \qquad (1A)$$

(see XP spectra analysis[4–8]). The final and some other similar and congenial relations have then been named *the equations of the latent storage and reversible spillover of the primary oxides* (Pt–OH, Au–OH)).[4–8]

Hypo-d-electronic transition metal oxides usually feature several altervalent states giving rise even to interactive mixed valence compounds, such as, for example, TiO$_2$/WO$_3$, TiO$_2$/Nb$_2$O$_5$, TiO$_2$/Ta$_2$O$_5$, or TiO$_2$/Nb$_2$O$_5$/CeO$_2$,[11] and then correspondingly increase the overall adsorptive water molecules dissociation[12,13] or latent storage and spillover effect of both H-adatoms and primary oxides (M–OH). The whole spillover and SMSI effect behave typical synergistic electrocatalytic properties and never any individual hypo-d-oxide enables that much as mixed altervalent composites. Such coinciding and interconnected events and phenomena have finally been perfectly and broadly tuned in mutual interfering phase, and enabled us to approach and substantiate the reversible electrocatalysts for the oxygen electrode reactions. Meanwhile, as it might be theoretically predicted, Magneli phase[4–8,14–17] impose even remarkably more pronounced synergistic Pt–OH(Au–OH) spillover electrocatalytic contribution.

The problem so far was in unattainable nanostructured Pt-bronze,[27,28] the catalytic activity of which exponentially increases with decreased Pt nano-size approaching maximum at monoatomic dispersion.[30] This requirement has now been fulfilled by the grafting im-plementation of Pt-acetylacetonate (Pt-acac) within col-loidal particles of peroxopolytungstic acid,[31,32] niobia (Nb$_2$O$_5$), tantalia (Ta$_2$O$_5$)[11] and ceria (CeO$_2$),[33,34] (Figure 3),[4–8] after thorough supercritical drying with liquid carbon dioxide. Such homogeneous and even distributions of nano-structured Pt(Au) particles, and such SMSI bonding effectiveness, so far were missing the experimental evidence in PEMFCs development. In other words, as the broader overall guiding conclusion, the higher the altervalent number even as the summed up value, the larger the spontaneous dissociative water molecular adsorption of hypo-d-(f)-oxide supports, and consequently so, the larger the latent storage of the primary oxides (Au–OH, Pt–OH), and finally, the faster the catalytic electrode reaction rate (ORR). Thus, the first approaches, based on the interactive hypo-d-oxide supported Pt electrocatalysts, initiated with Pt-bronze.[31,32] Meanwhile, there arises even much more pronounced multiple Magneli phase electrocatalytic effect with many advantageous features of anatase titania, which otherwise remarkably prevail in heterogeneous catalysis. The point is that various oxide supports (Al$_2$O$_3$, SiO$_2$, ZnO) so far have been employed as catalyst supports in heterogeneous catalysis,

while **_only_** hypo-d-(f)- individuals and composites, ones more, ones less, provide synergism in the latent storage and spillover of the primary oxide (Pt–OH, Au–OH), according to the reversible mechanism of the ORR and OER for electrocatalysis displayed in the present paper (Scheme 1).

Some Additional Subtle Potentiodynamic and Polarization Scans

The substantial interest now is primarily focused on the actual mixed interfering Pt oxide coverages at various points within the characteristic potentials close to the open circuit value and mostly along the reversible potential range of low Tafel line slopes. Under such sharply defined polarization circumstances of *a priori* existing and broadly imposed the strong **_reaction polarization_** range of the primary oxide (Pt–OH→0) disproportionation into the irreversible, rather stable, strongly adsorptive bonded and highly polarizable (Equation 2) surface oxide (Pt=O→1), electrocatalytic activation certainly might imply the spontaneous external reversible latent storage and continuous spillover supply of the missing sources of the former for the entire reversible reaction (Equation 3) to occur continuously. Otherwise, there is no other available source of the former for the reversible reaction with the latter. In such a context, some additional subtle potentiodynamic survey of fundamental significance, along with polarization properties of some typical and characteristic novel interactive hypo-d-(f)-oxides supported nanostructured Pt(Au) electrocatalysts for both the ORR and OER,[4–8] enable to select some diagnostic kinetic criterions, otherwise decisive on the way towards the reversible oxygen electrode features, revealing from their Tafel plots: (i) Nano-dispersed Pt/C clusters (10 wt. % Pt) non-interactive adhering upon sol-gel developed indifferent nano-particulate E-tek, Inc., Vulcan-XC-72 carbon (240 m^2/g) carrier and current collecting species, considered for the classical issue of such an electrocatalytic activity comparison; (ii) The interactive supported nanostructured Pt particles upon both the extra stable and electron conductive (300 − 1,000 S/cm), ceramic Magneli phases (Ebonex®), Ti$_n$O$_{(2n-1)}$, in average Ti$_4$O$_7$, usually defined as a shared rutile structure, accommodating the oxygen suboxide deficiency in the structure by the formation of crystal shared planes along the **n**th layerlike plane of octahedron, so that Ti$_4$O$_7$, has one TiO for every three TiO$_2$ layers; (iii) Advanced interactive selective grafted and homogeneously distributed nanostructured Pt clusters down to the prevailing (2.2 ± 0.2 nm) nano-size, upon the optimized structure of mixed valence hypo-d-oxide compounds (Pt/Nb$_2$O$_5$,TiO$_2$/C), and even further extended (iv) composites with hypo-f-oxides (Pt/Nb$_2$O$_5$,CeO$_2$,TiO$_2$/C, including doped GdO$_2$, HoO$_2$, and/or LaO$_2$ itself), and their relative combinations of extra high stability and remarkable electron conductivity (300 S/cm, and more), too. Such
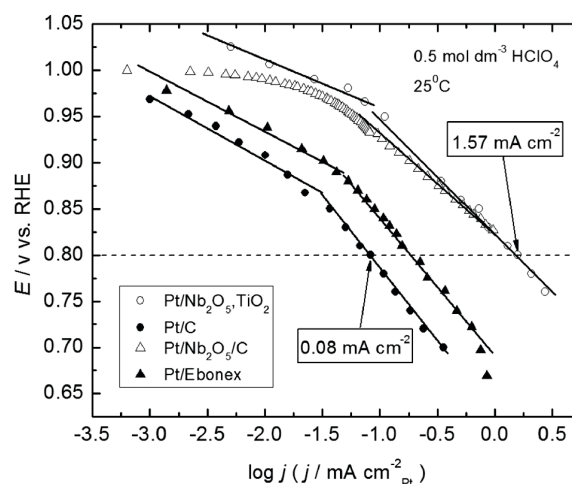
Figure 5. Tafel plots for the cathodic ORR scanned on RDE in 0.5 M HClO$_4$ solution at 25 °C for E-tek, Inc., Pt/C (Vulcan XP-72, closed circles); Pt/Ebonex (Magneli phases, closed triangles); Pt(10 wt. %)/Nb$_2$O$_5$ (20 wt. %)/C (70 wt. %) (open triangles); and Pt/Nb$_2$O$_5$ (5 mol. %),TiO$_2$ (95 mol. %) (open circles)(N. V. Krstajic measured and plotted).

comparable diagnostic Tafel polarization interdependences distinctly displays Figure 5, with differences of more than an order of magnitude in the electrocatalytic activity for the ORR that arises **_only_** as the result of different hypo-d-f-oxide type of interactive catalyst supports, relative ratios of their amounts *vs.* the same nanostructured metallic part of the catalyst (Pt), and their corresponding SMSI.[4–8]

A specific potentiodynamic survey has then been focused on the actual mixed interfering and kinetically decisive Pt–OH/Pt=O ratios (Equation 3), at selected points within the characteristic potentials close to the open circuit value and all along the reversible potential range of low Tafel line slopes (mostly bellow 30 mV/dec, Figure 5). In such a respect, each the preconditioned electrode at 0.20 V(RHE), was then successively potentiostated at all these selected potential values (Figure 6(a,b), for fixed time period (30 s), and afterwards, to avoid and mask all slow reaction steps, these were further exposed to the high sweep rates in the striping voltammetry scans, from such selected initial reversible values, down to 0.0 V (RHE).

The main conclusions then have been that Pt electrodes, both plain and interactive supported upon hypo-d-oxides, have been covered by mixed (Pt–OH, Pt=O) oxides (besides many other experimental methods, *in situ* and *ex-situ* XPS confirmed,[6–8,35–37] while at higher irreversible polarization (120 mV/dec), they were completely deprived from such adsorptive layers. In other words, within the reversible range, the ORR is associated with and **proceeds upon and from mixed oxide covered Pt surface**, as the interfering self-catalytic spillover electrode process, (Equation 3), otherwise known as the fastest

reaction step,[9] like at its open circuit potential. Meanwhile, the oxide-free Pt surface, like monolayer Pt=O covered electrode, imposes much higher polarization for the direct electron transfer electrode reaction, (Figure 1, Equation 2), to occur and proceed.[5–8,35–37] Thus, the conclusive observation has now been that *Pt oxides, primarily the primary oxide, (Pt–OH, Au–OH), play the same spontaneous self-catalytic role to establish the ROE properties*, as the spontaneous hydrogen (Pt–H) adsorption does and means for the RHE. In fact, the leading idea consists now from the extension of the reversible Tafel plot for the ORR all along the potential axis down from or up to the thermodynamic value (1.29 V *vs*. RHE) that implies enriched spontaneous external latent Pt–OH storage and continuous spillover supply all along in both scan directions, and particularly within the critical potential range (Figures 1 and 3). Namely, so far the problem and obstacle were the initial highly reaction polarizable potential range, (Pt–OH→0, Equation 2), of strongly adsorbed monolayered (Pt=O→1) and at the same time missing the Pt–OH, which cannot be supplied from aqueous solution, but only as the adsorptive surface species. Fortunately, the Vitadini[12,13] spontaneous dissociative adsorption of water molecules upon hypo-d-(f)-oxides, optimal structured Magneli phases (Ti_4O_7), and more particularly on their mixed valence compounds (of high altervalent components), at the same time means and provides the first main step of enriched reversible latent storage and spillover of primary oxides (Pt–OH, Au–OH). The amount of charge (Figure 6(a,b)) imposed during such Tafel scans, and determined by their peak integration, proved that the surface coverage of Pt interactive supported on Magneli phases (Pt/Ti_4O_7), by adsorptive oxide species was for an order of magnitude lower than on nanostructured, but non-interactive supported Pt/C, because of remarkably higher catalytic activity and/or distinctly increased the reaction rate at the same potential values, and both were decreasing with successive negative potential values of polarization, the adsorption conditions being Langmuirian in all issues. These rather specific potentiodynamic measurements consequently and even more clearly show that the ORR upon Pt/Ebonex Magneli phases starts and finishes at remarkably more positive potential values (1.05 down to 0.86 V, *vs*. 0.95 down to 0.8 V, all *vs*. the RHE, Figure 6), relative to polycrystalline Pt metal and/or nanostructured Pt/C;[5,6] whereas the other two congenial issues (iii & iv) initiate with 1.29 V as the completed reversible property of the ROE (Figures 2 and 3), and have been the ones of main substantial conclusive remarks on the way towards the ROE (electro)catalysts. These afford and enable the reliable link between the reversible and *polarized* oxygen electrode properties.
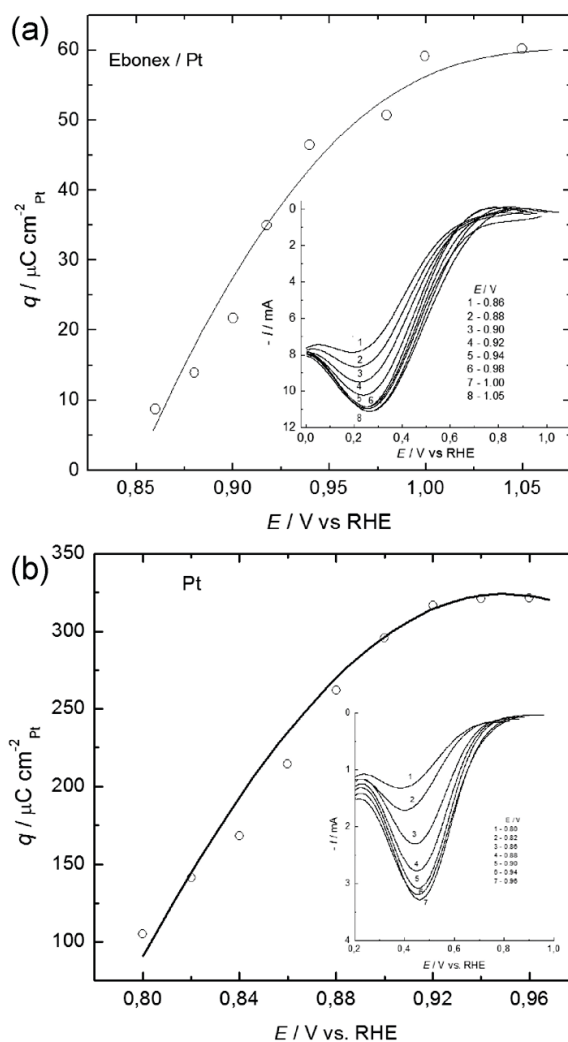

Figure 6. (a) Charge density (q) that required oxygen species (Pt-OH/Pt=O) for their reduction, presented as a function of potential for the Pt/(Magneli phases) (5 mg) electrode; same as in Figure 5. The insert shows potentiodynamic I *vs*. E relations scanned from different initial potentials (hold) with sweep rate of 5 V s^{-1}.)(N. V. Krstajic conceived and plotted). (b) The same as in Figure 6a, but for polycrystalline Pt metal.

In such a respect, the guiding concept implies homogeneous nanostructured distribution and selective grafting while interactive hypo-hyper-d-d-interelectronic bonding of Pt(Au) nano-clusters upon various individual and preferably mixed valence hypo-d-oxide supports (Figure 3), taken for the reversible external interconnected latent storage and spillover Pt–OH (Au–OH) sources (Scheme 1), primarily Nb_2O_5,TiO_2 (or Ta_2O_5,TiO_2), MPs and their composites because of much advanced both the stability and electronic conductivity. In such a constellation, nano-particles of solid oxides and Pt establish the SMSIs,

the ones of strongest in the whole chemistry, together with the electron conductive transfer, while external surface of hypo-d-oxide deposit undergoes spontaneous dissociative adsorption of water molecules and thereby becomes, along with continuous further water vapor supply (Scheme 1), the renewable and dynamically almost unlimited spontaneous latent storage and spillover source of the Pt–OH.

Poetic (Electro)catalytic World of Magneli Phases and Its Unique Advances in Electrocatalysis for Oxygen (ORR & OER) Electrode Reactions

The 20th century has finally brought Dimensionally Stable Anodes[38] (DSA), along with other titanium metal based equipment in chemical industry. The entire and surface stability provides the insulating, resistive and spontaneously growing thin layer of TiO_2, while the catalyst and current carrier roles and collection undertakes metallic titanium itself, in conjunction with individual or mixed noble metal oxide ($Ti/RuO_2,TiO_2$, and/or $Ti/RuO_2,PtO_2,TiO_2$) layers. Although rather slowly growing, the insulating TiO_2 layer, after many (18–24) months of electrode operation, definitely succeeds to separate metallic Ti from the catalyst (RuO_2) coating, that way ceasing the entire electrocatalytic activity. Sand blasting removes the grown otherwise negligible amount of strong insulating layer from clean Ti metal, while the catalyst recoating comes as the layers of painted $RuCl_4$ in anysol solvent, whereas the reactivation itself takes place in the oxygen furnace at moderate heating (320 °C). This is the point and the substantial difference relative to the congenial issues of hypo-d-(f)-oxides, in particular Magneli phases,[16,17] as various interactive catalytic supports.

Since the core substance of novel bifunctional electrocatalysts represents the interactive hypo-d-(f)-oxide support, primarily operating as the latent storage and generating unit cites for the primary oxide (Pt–OH, Au–OH) spillover, the following properties have been *a priori* implied: (i) Extra high stability in particular when interacting with hyper-d-metals, since then even hypo-d-(f)-oxides exchange d-(f)-electrons and behave as d-metals themselves; (ii) Advanced n-type electron conductivity and interelectronic bonding; (iii) Both surface and bulk matrix membrane type ionic mass transfer associated with the primary oxide spillover widespreading over metallic nanostructured catalyst, the entire focus being primarily posed on advanced Magneli phases (MPs), as the most promising electrocatalyst interactive supports.

In such a respect, the mine decisive step towards spontaneous latent storage and rather fast spillover widespreading phenomena of the Pt–OH(Au–OH) is the consequence of a strong first principle thermodynamic confirmed evidence (Density Functional Calculations, DFC)

by Vittadini *et al.*,[12,13] that water *molecules undergo prevailing spontaneous dissociative adsorption on anatase (101), and even rutile titania,* and more so on the higher altervalent hypo-d-oxides[4–8,13,14] of tungsten bronze type, molybdenum, tantalum, niobium, yttrium and/or cerium, *etc.*, as the *general oxophilicity properties of hypo-d-metal oxides*. In addition, the simultaneous first-principles molecular-dynamic showed the existence of a mechanism for thermodynamically favored spontaneous dissociative adsorption of water molecules even at low coverage of oxygen vacancies[39] of the anatase (101) surface,[12,13] and consequently even more so at the MPs,[16,17] as substantially suboxide structure significant both as highly bulk electronic conductive matrix (up to and even more than 1,000 S/cm),[17] perfect membrane type surface and bulk matrix transferring hydroxide and other ionic species,[18–20] and the interactive (SMSI)[10] hypo-d-oxide type catalyst support. Actually, it has for longer been known that *TiO_2 can easily accommodate suboxide type of oxygen vacancies and deficiances, and in broader sense a wide range of* various *substoichiometries,*[13,14] along with *reducing defects in TiO_2. MPs then can be described as resulting from a regular arrangement of crystallographic shear (CSh) planes in oxygen-deficient rutile structure*, the latter being stable for intermediate (MPs hybrid) stoichiometries between Ti_2O_3 and TiO_2, as two interfering states of the MPs steucture.

The interactive supported nanostructured Pt particles upon both the extra stable and electron conductive, ceramic Magneli phases (Atraverda Ebonex®), $Ti_nO_{(2n-1)}$, in average Ti_4O_7, usually defined as a *shared rutile structure*, accommodating the *oxygen suboxide deficiency* in the latter by the initial local edge formation of *crystal shared planes* (CSh) along the nth layerlike plane of octahedron, so that Ti_4O_7, has accommodated one suboxide or vacant TiO for every three TiO_2 layers. The latter would be stoichiometric formula presentation for the mass-balance MPs occurring from anatase and/or rutile titania by a simple thermal reduction, transferring and existing as the interfering dynamic (hybrid) state (4 $TiO_2 \Leftrightarrow Ti_4O_7 + O$), lake a prevailing integral static or interfering step otherwise including and implying multiple dynamic suboxide (and multistate steps) (phase diagram).[40]

Majority of papers denote Ti_4O_7, as a prevailing average in MPs. Meanwhile, since accommodated oxygen suboxide deficiency CSh at the same time defines the catalytic activity, the latter taking its optimal or maximal value, when n → min, and coincides with the nominated average value in general formula, ($Ti_nO_{(2n-1)}$), while the latter keeps its overall meaning and significance.

There now almost self-imposes the question of substantial fundamental sense and significance: What is the innate thermodynamic self-catalytic driving force

enabling anatase and rutile titania phase transfer from substantially insulating into Magneli phases of extra high stability and substantially high metal or n-type electronic conductivity by simple _thermal_ treatment? In fact, for the same mass amount or composition between (anatase and/or rutile) titania _vs._ Magneli phases, and unaltered stoichiometry, such dramatic, highly prevailing changes in the enthalpy thermodynamically impose and result from the _definite entropy decreased values_, when altering from high disorder of titania insulation to the MPs extra high ordered electron conductivity, their dramatically advanced new crystal lattice, and consequently so, some other properties, such as their catalytic gain when transferring from the ones to another (CO tolerance on Pt/TiO_2 and/or $Pt/(Ti_4O_7)$).

TiO$_2$ is an extra important technological material of the new age now with a broad range of applications, including photocatalysis in photo-voltaics, mostly for hydrogen fueled sustainable L&MT PEMFCs, and solar energy conversion, heterogeneous catalysis (Au/TiO$_2$ in CO tolerance), electrocatalysis {(Au/(Ti$_n$O$_{(2n-1)}$)), ORR, OER}, electrodes for electrochemical (chlorate and chlorite production) cells, and novel memristor switching memories. In particular, memristors are based on a _resistive switching phenomenon_ which in TiO$_2$ has been _associated with a spontaneous local phase transformation to a Magneli phases (MPs)_,[14–16] Ti$_n$O$_{(2n-1)}$, otherwise resulting from a simple _thermal reduction of the original TiO$_2$_ matrix. Such a spontaneous memristor phase transformations between TiO$_2$ and Ti$_4$O$_7$ are the best confirmation for the entropy change as the driving force.

Within the rich titanium-oxygen phase diagram,[40] homologous series of compounds occur, among which the mixed-valence Magnli phases are decisively important representatives. _MPs then can be described as resulting from a regular arrangement of crystallographic shear (CSh) planes in oxygen-deficient rutile structure_.[13–15] These structures are stable for intermediate stoichiometries between two main inter-valence states, Ti$_2$O$_3$ and TiO$_2$, and most significant for the Pt–OH(Au–OH) latent storage and spillover.

Plate MPs are now employed not only as interactive supports, but straight as catalytic electrodes in chlorate cells and Li batteries (Atraverda, Ebonex®), since under such circumstances they themselves behave satisfactory polarization properties without any metallic plain, micro-, or nanostructure. Thence, _vice versa_, when talking about the stability of MPs, it is enough and fascinating just to infer that these are used now as electrocatalytic anodes in industrial chlorate cell production.

Since MPs growth initiates with local phase transformations, CSh, including simple _local defects and various sub-states, sub-stoichiometries and involving_ _regular agglomerations, all interfering between the two main inter-valence states, (TiO$_2$ vs. Ti$_2$O$_3$), these enable a comparable analysis with cyclic voltammetry_, as concerns latent storage and spillover, TiO$_2$ _vs._ MPs, to distinguish probable from impossible, and define the entire system.

Interchangeable Interfering Reversible and Polarizable Oxygen Electrode Reactions

In general, when nanostructured Pt(Au) electrocatalyst selectively interactive grafted upon hypo-d-(f)-oxide supports, exists with the hydrated external surface and/or wet internal bulk matrix state (Scheme 1), then consequently exhibits enriched Pt–OH(Au–OH) latent storage, as the feedback oxophilicity effect and property. The corresponding primary oxide then continuously features its renewable spillover, simply by water vapor supply (surface phenomena, no concentration polari-zation), and further continuously yielding spontaneous adsorptive dissociation of aqueous species, so that the reversible anodic oxygen evolution (Equation 4) now takes place straight from pronouncedly high and also the highly reversible Pt–OH (Au–OH) adsorptive peak capacities, (Figures 1–3),[1–8]

$$4Pt-OH \Leftrightarrow O_2 + 2H_2O + 4Pt + 4e^- \qquad (5)$$

and, thence, at the thermodynamic equilibrium (ROE) potential value. Quite on the contrary, in classical issues (Figure 1), the latter occurs from the strong irreversibly deposited and highly polarizable monolayer of the Pt=O, (Equation 2), and thereby, while being deprived from primary oxides, at rather high anodic overpotential values,–

$$2Pt=O \Rightarrow O_2 + 2Pt + 4e^- \qquad (6)$$

The same, _vice versa_, consequently alternately occurs both in these reversible and/or irreversible states, as concerns the ORR, all along the reverse cathodic scan and polarization (Figures 1–3). The transient between the reversible and irreversible status features some sharp thresholds both as a function of hypo-d-(f)-oxide unit content[11] and/or wetness percentage (Figures 1–3),[7] and substantially reflects the Pt–OH (Au–OH) properties (present or absent) for the oxygen electrode reactions. In such a context, plain and non-interactive supported Pt (Pt/C), in the absence of primary oxides, and thereby established or _a priori_ existing the broad reaction polarization range, by no means can feature the overall reversible oxygen electrode properties within the whole potential axis, in between of the hydrogen and oxygen evolving limits. Thus, there exists either the reversible behavior in the presence or continuous external supply of primary oxides, or highly irreversible properties in the

absence of the latter, (Pt−OH→0, Au−OH→0), and this is the substance for Pt and Au electrocatalytic properties!

In such a context, the simple stoichiometric combination of Equation 1 and Equation 4, reveals that the overall reversible anodic oxygen evolution initiates from water molecules (Equation 1), and obeys the auto- or self-catalytic Ertel framework,[24] with the general oxidation mechanism based on and catalyzed by M−OH species, or the primary oxides as the main interfering electrocatalytic species, and substantially takes place at the reversible oxygen potential value; the same in the reverse cathodic ORR scans. However, when oxygen evolving initiates from Pt(Au) monolayer covered by the strongly adsorptive and polarizable surface oxide (Pt=O. Au=O), the anodic, and reverse cathodic reaction have both to overcome remarkable overpotentials (Equation 5, adjoined with Equation 2). This is the substance and difference as concerns the irreversible plain (Pt,Au) and non-interactive supported Pt/C(Au/C), and/or the enriched latent storage and continuous external spillover feeding of the primary oxide for interactive hypo-d-(f)-oxides supported Pt electrode.

In fact, the just displayed analytical survey and experimental evidence belong to the crucial arguments that the interfering oxide ratio [Pt−OH]/[Pt=O] means the optimization key, (Equation 3), to approach the ROE and corresponding electrocatalytic effects enabled by the primary oxide latent storage and spillover. In such a sense spontaneous adsorptive dissociation of water molecules,[11,12] that substantially means and defines the latent storage of primary oxides, results with transferable hydroxyl ions (membrane type migration),[18–20] which when transfer their prevailing ionic charge to metallic catalyst, effectively and substantially become dipoles.[21]

Anodic HCHO Oxidation and Primary Oxide Spillover

Cyclic voltammetry has been employed to investigate and characterize the potential dependent growing adsorptive anodic and reverse desorptive cathodic Pt−OH surface properties, because potentiodynamic spectra afford the most illustrative, versatile and reliable scanning method for studies of heterogeneous electrode reactions in aqueous media all along the potential axis between hydrogen and oxygen evolving limits. Since the heterogeneous reaction of formaldehyde oxidation with Pt−OH, and in particular Au−OH, proceeds as a fast reversible anodic process mass transfer limited, and since HCHO is soluble in all ratios in aqueous media, the primary oxide generation rate and its yielding spillover, have primarily been investigated by potentiodynamic spectra within the broader concentration range and between hydrogen and oxygen potential evolving limits (Figure 7(a,b)). Their anodic reaction starts immediately after (or even within) UPD H-adatom desorption,
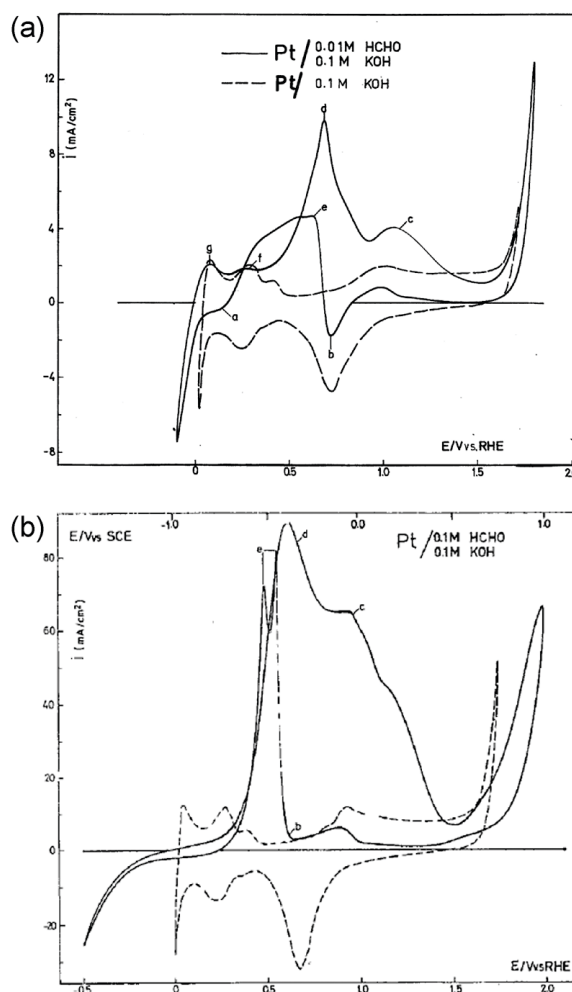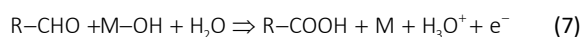

Figure 7. Cyclic voltammograms scanned on a polycrystalline Pt wire electrode in alkaline (0.1 M KOH, dashed lines) solution and in an admixture of formaldehyde (0.01 M (Figure 2a) and 0.1 M HCHO (Figure 2b), full lines) at 200 mV·s⁻¹ sweep rate between hydrogen and oxygen potential evolving limits. Labels: (a) reversible hydrogen adsorption peak; (b) irreversible Pt surface oxide (Pt=O) desorption peak; (c and d) successive peaks of anodic aldehyde oxidation; (e) sudden sharp current jump and reverse peak of repeated HCHO oxidation in the course of successive cathodic scan; (g and f) reversible H-adatoms oxidation and desorption peaks, respectively (Reprinted with permission from Ref. [7]. Copyright (2014) American Chemical

$$R-CHO + M-OH + H_2O \Rightarrow R-COOH + M + H_3O^+ + e^- \qquad (7)$$

where for the particular HCHO issue, apparently proceeds further all along the DL charging/discharging pseudo capacity range in acidic or alkaline solutions.

Such for more than an order faster heterogeneous anodic reaction is able to postpone within unusually long

potential range the recombination of the primary (Pt–OH), into the more polarizable, more stronger adsorptive, more irreversible, and more stable surface oxide (Pt=O), (Equation 2), simply by faster removal of the entire amount of successively generated Pt–OH, that way being deprived for other reactions. Formaldehyde oxidation starts exactly at its reversible potential (0.32 V *vs*. RHE), in vicinity of the usual lower DL charging potential limits, even merges with the second UPD desorption peak of H-adatoms, and extends as an exaggerated broad twins peak all along the anodic scan, nearly until the beginning of OER (Figure 7a). In the same sense, the anodic Pt–OH striping CO oxidation on composite hypo-d-oxides interactive supported Pt or Pt,Ru catalysts takes place even within the usual interval of UPD H-adatoms desorption (Figure 7, Ref. [21]), and dramatically exceeds the activity of composite plain intermetallic electrocatalysts (Ru,Pt or Ru–OH/Pt transfer-ring and reaction effect). In other words, Pt–OH arises available for reaction not only within its nominal reversible adsorption/desorption peak limits in regular mineral acid or alkaline aqueous solutions, Figure 1, but depending on the reactant (HCHO, HCOOH, CO, *etc.*) concentration, affinity and its actual reaction rate, along an unusually broad and striking extendable potential range. Meanwhile, as the link of DL charging/discharging pseudo-capacitance, it actually extends and appears available all along the whole potential axis of cyclic voltammograms. Such an unusually broader charge pseudo-capacity area (Figure 7(a,b)), usually features all the properties of typical under- and over-potential oxidation (UPO, OPO) peaks, in particular when compared with cathodic UPD properties of H-adatoms on Pt, Au and various other transition metals. Such specific cyclic voltammograms even more clearly and convincingly reveal the entire phenomenon of the interference between Pt–OH and Pt=O, illustrate and testify for the imposing and/or suppressing reaction polarization by the dispropor-tionation (Equation 2), along the distinctly and striking broader potential range. In other words, such cyclic voltam-mograms on a visual manner show that Pt=O peak grows or reduces only as the result of the Pt–OH reactive presence or absence, thence reflecting their actual interactive inter-ference. There even often reveals itself the longer zero cur-rent backward scan traversing, apparently within the longer absence of the primary oxide (Pt–OH) for interference with Pt=O, or missing the latter for simple cathodic desorption, and then there arises the sudden hysteretic reverse anodic jump at the potential of its reappearance, Figure 7(a,b). Such a potentiodynamic interplay between the primary (Pt–OH) and surface (Pt=O) oxides in the presence of and enabled by the controlled heterogeneous catalytic HCHO reaction, is of remarkable fundamental theoretical sig-nificance in the present study, when dealing with substantiation and optimization of composite electro-catalysts for the OER (ORR & OER).

Stepwise extension of positive potential limits toward the oxygen evolution reaction (OER), in the presence of HCHO, clearly shows (Figure 7(a,b)) the absence and/or distinctly reduced adsorptive Pt=O growth almost until oxygen starts evolving. Thence, during the reverse potential scan toward the HER, as the result of the latter, there arises and finishes the Pt=O desorption much earlier and of dramatically reduced charge capacity, than nominally in the simple (the absence of HCHO), acidic or alkaline solutions, Figure 1. As the result, the appearance of a characteristic sharp backwards growing anodic current jump and the corresponding peak in the reverse potential sweep direction, then testifies for the hysteretic (cathodic sweep, anodic peak) aldehyde oxidation within the former DL charging/discharging range, and this way reflects the specific and highly interactive properties of the Pt–OH. In other words, as a corollary, there is no anodic aldehyde, alcohol, their simple acids, and even CO oxidation, nor the ORR, upon any M=O (Pt=O, Au=O) covered metal surface prior to the potential of molecular oxygen evolution, when the latter becomes broken, and/or only upon the prevailing Pt–OH spillover deposits.

Namely, since aldehydes are often soluble in aqueous media almost in all ratios, their voltammograms at high contents feature imprinted extremely high both charge capacities and limiting currents at their peaks (Figure 7b), and thereby testify for almost unlimited reversible reaction rates (Equation 1), as long as diffusional mass-transfer supply provides enough reacting species. Even more so, for interactive supported Pt and Au upon higher amounts of altervalent hypo-d-oxides and their mixed valence compounds, since these behave as highly enriched latent storage capacities of primary oxide spillover sources, and when compared with the CO removal from the active electrode surface of Pt(Au), become particularly pronounced.

This is the cause and reason why within the reversible part of Tafel plots electrocatalytic metal (Pt,Au) surface is always covered by the interacting Pt–OH/Pt=O species, and naturally tends to impose the reversible oxygen electrode properties, and these are the experimental evidence that the optimal catalytic rate implies their optimal ratio.

In such a context, meanwhile, one of the most outstanding observations has been that cyclic voltammograms of both formaldehyde (Figure 3, Ref. [41]) and formic (muriatic) acid (Figure 3, Ref. [42]) anodic oxidation distinctly differ upon plain (Pt) or non-interactive carbon supported platinum (Pt/C), and the same, but more or less enriched and more exposed hypo-d-(f)-oxide support surfaces. Such a dependence, meanwhile, passes through certain maximum, since the increasing partial amount of hypo-d-(f)-oxides finally too much separates and

isolates nanostructured Pt(Au) particles from each other. In such a context, at specific amounts of these interactive hypo-d- (Pt/Ta$_2$O$_5$/C,[41] and/or hypo-f- (Pt/CeO$_2$/C[42]) oxide supports, accounted per available metal electrode surface, the electrocatalytic activity increases remarkably, but not endlessly. In other words, the all parameters and conditions being kept the same, the reaction rate becomes dramatically different upon various supported electro-catalysts in their hypo-d-(f)-oxide amounts and/or exposure, as the result of distinctly different the additional Pt–OH spillover feeding and spreading effects, and as the only distinctly imposed difference. Such a conclusive observation belongs to the main experimental arguments to prove the theory of the M–OH interfering self-catalytic spillover contributions in electrocatalysis of aqueous media, (Equation 3),[6,7,41,42] finally providing the ROE behavior and properties, and traced the way and entire approach for its substantiation. In such a respect, cyclic voltammograms entirely deeper enlightened and more revealed the interfering spillover reaction impact properties of the Pt–OH.

Potentiodynamic Scans of Primary Oxide Latent Storage of Pronounced Capacities and Electrocatalytic Spillover Spreading

Some intermolecular compatible hypo-d-oxide mixed valence architecture (Pt/WO$_3$,TiO$_2$/C; Pt/Nb$_2$O$_5$,TiO$_2$/C; Au/WO$_3$,TiO$_2$,Ti$_4$O$_7$/C; Au/Nb$_2$O$_5$,TiO$_2$,Ti$_4$O$_7$/C), as the interactive catalytic submonolayer supports of high altervalent number or capacity, and highly developed and fixed available exposed surface area by the liquid CO$_2$ supercritical drying, have been investigated by potentiodynamic scans to reveal both the primary oxide latent storage and resulting spillover yielding properties, along with same for H-adatoms. In this respect, cyclic voltammograms scanned at low threshold moisture content of He stream (just enough to enable basic electrode processes to occur and proceed), insufficient for WO$_3$ (or Nb$_2$O$_5$ and/or TiO$_2$) hydration, repeatedly reveal similar potentiodynamic spectra characteristic for indifferent carbon (Pt(Au)/C) support, or plain Pt itself (Figure 3), but with high double layer charging capacity, because of the accompanying parallel charging of Vulcan carbon particles beside the metal (with correspondingly large charge value, Q$_{DL}$= 1.07 C).

In contrast to such fairly common occurrences, a continuous supply of saturate water vapor in the He stream at higher saturation temperature (80 °C), imposing condensation (Boudart spillover precondition[22,23]), and leading to the appearance of wet titania-tungstenia mixed valence oxide composite, along with spontaneous dissociative adsorption of water molecules all over its exposed hypo-d-oxide surface,[12,13] as the interactive

catalytic support, has been accompanied by the unusual phenomenon of a dramatic expansion of two reversible pairs of peaks of both the primary oxide (Q$_{Pt–OH(a)}$ = Q$_{Pt–OH(c)}$ = 1.453 C), and H-adatoms (247 *vs.* 47 mC cm^{-2}, or in the ratio of about 5.3:1) for chemisorptive deposition and desorption (Figure 3), like a DC pseudo-capacitance of extremely developed electrode surface. Since these are highly reversible and evidently behave pronounced the latent Pt–OH storage (*cf.* Refs. [4–8,11]), they keep the same their extents even after multiple and repeating number of cycles at any other time. The latter have both been of unusually high spillover charge and discharge capacity values (or, the latent storage itself), and for Pt–OH (UPD and OPD) shifted towards both much more negative and far positive potential limits, in common with Figure 6(a,b), and discussion thereon. In fact, two distinctly different cyclic voltammogram shapes and charge capacities (Figure 3), appear only as the result of the difference in water vapor supply, all other parameters being unaltered the same, and as the effect of the equivalent dipole (Pt–OH) charging and discharging of the double layer, since nothing else takes place in between. The entire effect of enormous reversible Pt–OH (Au–OH) peak growth or, the latent Pt–OH charge storage capacity has been the result of dramatically enlarged spontaneous adsorptive dissociation and even monolayer condensation of water molecules upon developed hypo-d-oxide surface and at much higher saturation temperature, as the measure of the latent storage extent and spillover rate of the primary oxide (Pt–OH, Au–OH), since again, nothing else was done and occurred.

Every cessation in the steam supply instantaneously imposes the sudden reversible shrinkage of both such rather exaggerated pairs of peaks down to the same initial potentiodynamic shape similar to the plain nanostructured Pt/C voltammogram spectra themselves. *Vice versa*, the renewed saturate water vapor feeding immediately leads to their former Pt–OH peaks and the same former charge capacities; namely, the effect later already noticed and scanned for formaldehyde[41] and formic acid[42] oxidation. Such an appearance without exception behaves as a typical reversible transient phenomenon by its endless altering repetition,[4–8,35–38] and never appears upon the plain Pt/C electrocatalyst, both wet and/or dry, nor with small and insufficient amounts of catalytic hypo-d-oxide supports.

The complementary interactive Ta$_2$O$_5$- and Nb$_2$O$_5$-based electrocatalytic supports[11] strongly reinforce just displayed potentiodynamic features of Pt/WO$_3$,TiO$_2$/C by the coinciding and congenial spectral behavior of their cyclic voltammograms: The distinct parallel growth of Pt–OH and H-adatoms adsorption and desorption peaks, reflecting their different accumulated latent charge capacities, as a function of the amount (charge density) of

interactive composite hypo-d-oxide deposits per unit of exposed electrode surface (Figure 4, Ref. [11]). In such a respect, for example, as the effect of much smaller d-ionic radius, Y_2O_3 much more does so, than Nb_2O_5, or WO_3. In fact, such Pt–OH latent storage growth (including the corresponding spillover effect) does not extend endlessly and usually passes over remarkably pronounced maximum in the ORR catalytic rate and activity (see Figure 9, Ref. [43], Savadogo[44,45]).

What is now the substantial difference between voltammograms in Figure 3, wet state, and Figure 7(a,b)? Even when mostly suppressed in the surface oxide (Pt=O) adsorptive growth (Figure 7(a,b)), the reversal backward cathodic scans on plain Pt proceed still highly polarized for about 600 mV with negligible or zero current, exactly corresponding to Figure 1. In other words, there is no stored Pt–OH on plain Pt to start the self-catalytic interfering reaction (Equation 3) of the ORR, or HCHO oxidation. However, on the hypo-d-oxide interactive supported Pt catalyst, the *a priori* latently accumulated initial storage of the primary oxide from the beginning is ready and available for the reaction with surface oxide, and thence continuously provides and spillover enhances the latter to proceed as the uninterrupted and extra fast reversible electrode reaction, as long as there is continuous water vapor supply. However, for the plain Pt (or Pt/C), the sudden hysteretic sharp anodic current jump (HCHO) in the course of reversal cathodic sweep (Figure 7(a,b)) rearises at and coincides with the classical position of the reversible peak for the Pt–OH growth, reflects the local interfering self-catalytic state at such potential range, provided by the repeated Pt–OH spillover growth (Scheme 1). This is the striking point and the core substance of the present study, while Figure 3, supported by Figure 7(a,b), are the best illustrative issues of the substantiated reversible electrocatalyst for the oxygen electrode reactions (ORR, OER), (Equation 3 and 4).

Two distinct and novel things and achievements are worth noting: (i) In the presence of spontaneously adsorptive dissociated water molecules upon hypo-d-(f)-oxide supports, as the latent stored primary oxides (Pt–OH, Au–OH), there is no more establishing of any reaction polarization and the former proceeds continuously and repeatedly, almost endlessly, even while taking rather high current values, and (ii) Anodic oxygen evolution takes place as the reversible electrode reaction, (Equation 5), and consequently so, at its reversible potential value, (ROE).

What is substantially different now and of unique difference, when compared with any other simple or congenial cyclic voltammograms? The main decisive property is that currents continuously keep their increased constant level values and/or smoothly change ahead from

them, while cycling and when there appear certain characteristic growing adsorptive and in the course of the reversal potential scan, corresponding desorption peaks, all along the entire potentiodynamic cycles, being dependent only on the actual constant water wetness value.

Striping Voltammetry Evidence for the Primary Oxide Latent Storage and Spillover

Striping voltammetry represents another indirect complementary experimental potentiodynamic evidence to scan and prove the primary oxide spillover effects in electrocatalysis. Interactive hypo-d-oxide supported and non-supported electrocatalysts (both Pt and RuPt) exhibit dramatically different activity for CO tolerance in LT PEMFC, and distinctly provide new additional cyclic voltammetry scanning spectra for the M–OH spillover effect.[4–7] Ever since Watanabe[46] has shown that Ru even at submonolayer core-shell deposit, or while alloying with Pt, shifts the primary oxide growth to a much more negative potential range and enables CO tolerance, the primary oxide spillover became of substantial significance for PEMFCs.[47] Similarly, the hypo-d-oxide supported Pt and Ru ($Pt/TiO_2/C$, $Ru/TiO_2/C$) in their behavior *vs.* these two plain and non-interactive supported metals (Pt/C, Ru/C) themselves, or even their interactive unsupported *vs.* the supported alloys, RuPt/C and $RuPt/TiO_2/C$, Figure 8, have distinctly different catalytic properties, too, the interactive alternatives featuring an even more advanced and much more pronounced primary oxide spillover and catalytic effect.[4–7] Such distinct and clearly pronounced peak charge capacity difference between the interactive and non-interactive hypo-d-oxide supported Ru advanced electrocatalysts, belong to the best experimental evidence for the primary oxide spillover effect extension by the latent storage. Since hypo-d-oxides, primarily anatase titania, zirconia and hafnia, and even more so tungstenia, niobia and tantalia, facilitate the spillover of M–OH, such facts clearly point to the advanced overall composite effect and advantages of membrane type OH^- - transferring within and over TiO_2, WO_3, Nb_2O_5, TaO_2, and in particular within their substantially wet networks of mixed altervalent catalyst supports, resulting in the speeded-up primary oxide effusion, relative to the plain non-interactive carbon (Pt/C).

In other words, while Ru metal itself facilitates both Pt–OH and Ru–OH spillover transfer (by the same mechanism, Ru–OH + Pt $\Rightarrow$ Pt–OH + Ru), even in the intermetallic non-interactive supported alloy RuPt composite electrocatalyst,[46,47] the supporting effusion effect of titania advances the same effect for more than 300 mV relative to RuPt/C catalyst (Figure 8). Anodic CO
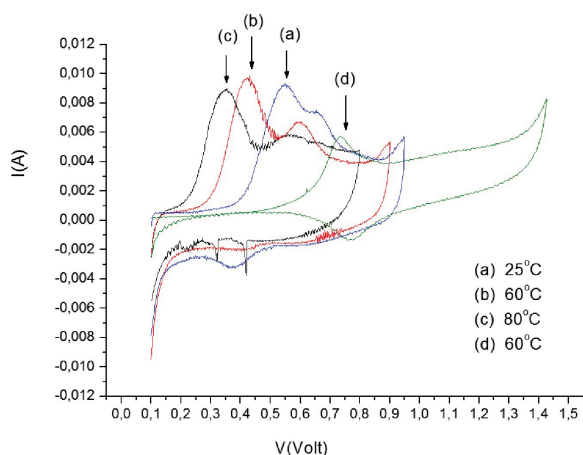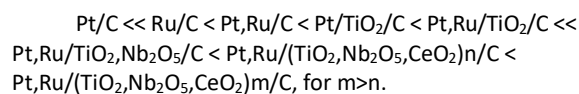
Figure 8. The striping voltammograms for CO desorption from supported 10 wt. % (0.4 mg cm^{-2}, 2 nm in average size, 1:1 atomic ratio Ru:Pt) RuPt/TiO$_2$/C electrocatalyst CO-saturated at three different temperatures: 25 (a); 60 (b) and 80 (c) °C, scanned at the scan rate of 2 mV s^{-1}; (d) the same stripping scans for CO desorption at 60 °C from un-supported 30 wt. % (0.5 mg cm^{-2}) E-tek RuPt/C electrocatalyst of the same RuPt nano-size, atomic ratio and load, and sweep rate 10 mV·s^{-1}; its CO saturation at 55 °C.

oxidation upon Ru,Pt/TiO$_2$/C starts even within the potential range of UPD desorption of H-adatoms and becomes much more pronounced in the charge capacity relative to Ru,Pt/C. Such an important result is one of the most significant confirmations of the present latent storage interactive and dynamic spillover catalytic model, as implemented in electrocatalysis for hydrogen and oxygen electrode reactions. In fact, cyclic voltammogram spectra of plain Ru feature a unique type of shapes and in both scan directions stepwise reveal more than any other individual transition metal various interrelating oxide states and their peak interdependances,[48] and with such overall potentiodynamic sequences are closer to the reversible properties for oxygen electrode reactions than any other d-metal.

Mixed anatase (and even rutile) titania, and in particular tungstenia, niobia and tantalia form intermolecular solid oxide solutions of a high altervalent capacity, compatible both in amorphous and crystalline forms of the edge sharing TiO$_6$ and the corner sharing WO$_6$ octahedrons, with pronouncedly increased electrochromic features even at high contents of the former.[49,50] In fact, highly charged W^{6+} cations, like Nb^{5+}, additionally favor the spontaneous reversible adsorptive dissociation of water molecules,[12,13] and thereby such electrochromic layers exhibit well defined ion exchange and electron conductive properties.[18–20] Thus, one of the fundamental contributions of the present paper is to show that prevailing

anatase titania in the form of a composite mixed valence catalytic hypo-d-(f)-oxide support with tungstenia (and/or even more so niobia, tantalia and molybdenia), behaves in a compatible way and regarding the (Pt/H$_{0.35}$WO$_3$ ⇔ Pt/W(OH)$_6$) bronze type equilibrium, so that the consequent reversibility features, the same properties as pure tungsten bronze itself, all of them have even further advanced by hypo-f-oxide ingredients (Ce,Gd,Ho,La, *etc.*)!

Now, the summed-up the CO tolerance conclusive view, experimentally assessed and plotted as the achieved striping rates of its removal, clearly display their dependence on the primary oxide latent storage (or its spillover rate):

Pt/C << Ru/C < Pt,Ru/C < Pt/TiO$_2$/C < Pt,Ru/TiO$_2$/C << Pt,Ru/TiO$_2$,Nb$_2$O$_5$/C < Pt,Ru/(TiO$_2$,Nb$_2$O$_5$,CeO$_2$)n/C < Pt,Ru/(TiO$_2$,Nb$_2$O$_5$,CeO$_2$)m/C, for m>n.

All these issues have further been consequently advanced in CO tolerance by MPs interference within the individual and composite hypo-d-(f)-oxide supports.

Titania (TiO$_2$) is almost unavoidable for hypo-d-oxide interactive catalytic supports, first since even low coverage of oxygen vacancies upon the anatase (101) surface[13] imposes the spontaneous adsorptive dissociation of water molecules[12] as the primary oxide latent storage. In addition, anatase and even rutile titania undergo spontaneous transfer to Magneli phases by simple thermal crystallization, when the impact of oxygen vacancies arises much more pronounced, and since the latter straight correlates with the spillover of the primary oxides, these become brought in a straight relation with the catalytic activity for the oxygen electrode reactions (ORR, OER).

The entire present study is mostly devoted to the primary oxide (Pt–OH, Au–OH), as the decisive reversible reacting species for the oxygen electrode reactions (ORR, OER). Meanwhile, there is a lot of recent papers entirely based on the primary oxide, though sometimes differently named and labeled.[51–78] The present approach has been revealed and displayed in details, while the analysis and comparisons with other contributions are stimulating afforded for the forth coming reviews and further original achievements in the field mostly looking for the L&MT PEMFCs.

REFERENCES

[1] B. E. Conway, *Prog. Surf. Sci.* **1995**, *49*, 331.

[2] H. Angerstein-Kozlowska, B. E. Conway, W. B. A. Sharp, *J. Electroanal. Chem*. **1973**, *43*, 9.

[3] B. E. Conway, H. Angerstein-Kozlowska, W. B. A. Sharp, B. E. Criddle, *Analytical Chem*. **1973**, *45*, 1331.

[4] J. M. Jaksic, N. V. Krstajic, Lj. M. Vracar, S. G. Neophytides, D. Labou, P. Falaras, M. M. Jaksic, *Electrochim. Acta* **2007**, *53*, 349.

[5] N. V. Krstajic, Lj. M. Vracar, V. R. Radmilovic, S. G. Neophytides, D. Labou, J. M. Jaksic, R. Tunold, P. Falaras, M. M. Jaksic, *Surf. Sci*. **2007**, *601*, 1949.

[6] J. M. Jaksic, G. A. Botton, G. D. Papakonstantinou, F. Nan, M. M. Jaksic, *J. Phys. Chem. C* **2014**, *118*, 8723.

[7] J. M. Jaksic, F. Nan, G. D. Papakonstantinou, G. A. Botton, M. M. Jaksic, *J. Phys. Chem. C* **2015,** *119*, 11267.

[8] G. D. Papakonstantinou, J. M. Jaksic, D. Labou, A. Siokou, M. M. Jaksic, *Adv. Phys. Chem*. **2011**. *2011*, 1-22, Article ID 412165.

[9] Y. Ma, P. B. Balabuena, *Chem. Phys. Lett*. **2007**, *440*, 130.

[10] S. J. Tauster, S. C. Fung, R. T. K. Baker, J. A. Horsley, *Science*, **1981**, *211*, 1121.

[11] Z. Awaludin, J. G. S. Moo, T. Okajima, T. Ohsaka, *J. Mater. Chem, A*. **2013**, *1*, 14754.

[12] A. Vittadini, A. Selloni, F. P. Rotzinger, M. Gratzel, *Surfaces. Phys. Rev. Lett*. **1998**, *81*, 2954.

[13] M. Lazzeri, A. Vittadini, A. Selloni, *Phys. Rev. B*. **2001**, *63*, Article no.155409.

[14] R. Ciancio, E. Carlino, G. Rossi, C. Aruta, U. Scotti di Uccio, A. Vittadini, A. Selloni*, Phys. Rev. B* **2012**, *86*, 114110.

[15] A. C. M. Padilha, J. M. Osorio-Guillen, A. R. Rocha, G. M. Dalpian, *Physical Chemistry B* **2014**, *90*, 35213-35217.

[16] A. Magneli, *Acta Chem. Scand*. **1959**, *13*, 5.

[17] F. C. Walsh, R. G. A. Wills, *Electrochim. Acta* **2010**, *55*, 6342.

[18] J. Livage, M. Henry, C. Sanchez, *Prog. Solid State Chem*. **1988**, *18*, 259.

[19] P. Judeinstein, J. Laivage, *J. Mater. Chem*. **1991**, *1*, 621.

[20] J. Livage, G. Guzman, **1996**, *84*, 205.

[21] M. T. M. Koper, R. A. Van Santen, *J. Electroanal. Chem*. **1999**, *472*, 126.

[22] H. W. Kohn, M. Boudart, *Science* **1964**, *145*, 149.

[23] J. E. Benson, H. W. Kohn, M. Boudart, *J. Catal*. **1966**, *5*, 307.

[24] S. Volkening, K. Bedurftig, K. Jacobi, J. Wintterlin, G. Ertel, G., *Phys. Rev. Lett*. **1999**, *83*, 2672.

[25] M. Date, M. Haruta, *J. Catal*. **2001**, *201*, 1221.

[26] M. Haruta, *Catal. Today* **1997**, *36*, 153.

[27] M. Haruta, *Chem. Record* **2003**, *3*, 75.

[28] T. Akita, K. Tanaka, S. Tsubota, M. Haruta, *J. Electron Microsc*. **2000**, *49*, 657.

[29] C. Lina, Y. Song, L. Cao, S. Chen, *ACS Appl. Mater. Interfaces* **2013**, *5*, 13305.

[30] M. Mavrikakis, P. Stoltze, J.K. Norskov, *Catal. Lett*. **2000**, *64*, 101.

[31] A. C. C. Tseung, P. K. Shen, K. Y. Chen, *J. Power Sources* **1996**, *61*, 223.

[32] A. C. C. Tseung, K. Y. Chen, *Catalysis Today* **1997**, *38*, 439.

[33] T. Masuda, H. Fukumitsu, K. Fugane, H. Togasaki, D. Matsumura, K. Tamura, Y. Nishihata, H. Yoshikawa, K. Kobayashi, T. Mori, K. Uosaki, *J. Phys. Chem. C*, **2012**, *116*, 10098.

[34] K. Fugane, T. Mori, D. R. Ou, P. Yan, F. Ye, H. Yoshikawa, J. Drennan, *Langmuir* **2012**, *28*, 16692.

[35] S. G. Neophytides, K. Murase, S. Zafeiratos, G. Papakonstantinou, F. E. Paloukis, N. V. Krstajic, M. M. Jaksic, *J. Phys. Chem. B*, **2006**, *110*, 3030.

[36] S. Zafeiratos, G. Papakonstantinou, M. M. Jaksic, S. G. Neophytides, *J. Catal*. **2005**, *232*, 127.

[37] J. M. Jaksic, D. Labou, G. D. Papakonstantinou, A. Siokou, M. M. Jaksic, *J. Phys. Chem. C* **2010**, *114*, 18298.

[38] K. E. Swider, C. I. Merzbacher, P. L. Hagens, D. R. Rolison, *Chem. Mater*. **1997**, *9*, 1248.

[39] E. Wahlstrom, N, Lopez, R. Schaub, P. Thostrup, A. Ronnau, C. Africh, E. Laegsgaard, J. K. Norskov, E. Besenbacher, *Phys. Rev. Lett*. **2003**, *90*, 026101-1.

[40] G. K. Samsonov, *The Oxide Handbook*, IFI/PLENUM, New York-Washington-London, 1973.

[41] J. Masud, M. T. Alam, T. Okajima, T. Ohsaka, *Chem. Lett. Japan* **2011**, *40*, 252.

[42] J. Masud, M. T. Alam, M. R. Miah, T. Okajima, T. Ohsaka, *Electrochem. Commun*. **2011**, *13*, 86.

[43] M. M. Jaksic, *Solid State Ionics* **2000**, *136/7*, 733.

[44] O. Savadogo, *Electrochim. Acta* **1992**, *37*, 1457.

[45] O. Savadogo, *J. Electrochem. Soc*. **1992**, *139*, 1982.

[46] M. Watanabe, S. Motoo, *J. Electroanal Chem*. **1975**, *60*, 267.

[47] J. C. Davies, B. E. Hayden, D. J. Pegg, M. E. Rendall, *Surf. Sci*. **2002**, *496*, 110.

[48] S. Hadzi-Jordanov , H. A. Angerstein-Kozlowska, M. Vukovic, B. E. Conway, *J. Electrochem. Soc*. **1978**, *125*, 1471.

[49] S. Hashimoto, H. Matsuoka, *Surf. Interface Anal*. **1992,** *19*, 464.

[50] S. Hashimoto, H. Matsuoka, *J. Electrochem. Soc.*, **1991**, *138*, 2403.

[51] D. Bejan, E. Guinea, N. J. Bunce, *Electrochim. Acta* **2012**, *69*, 275.

[52] D. Bejan, J. D. Malcolm, L. Morrison, N. J. Bunce, *Electrochim. Acta* **2009**, *54*, 5548.

[53] R. E. Fuentes, B. L. Garcia, J. W. Weidner, *ECS Transactions* **2008**, *12*, 239.

[54] A. R. Kucernak, G. J. Offer, *Phys.Chem.Chem.Phys*, **2008**, *10*, 3699.

[55] G. Chen, S. R. Bare, T. E. Mallouk, *J. Electrochem. Soc*. **2002**, *149*, A1092.

[56] M. Suh, P. S. Bagus, S. Pak, M. P. Rosinek, J. H. Lunsford, *J. Phys. Chem. B*, **2000**, *104*, 2736.

[57] Y. Luo, A. Habrioux, L. Calvillo, G. Granozzi, N. Alonso-Vante, *Chem.Phys.Chem*. **2014**, *15*, 2136.

[58] Bokhimi, A. Morales, O. Novaro, T. Lopez, E. Sanchez, R. Gomez, *J. Matter. Res*., **1995**, *10*, 2788.

[59] F. Tian, R. Jinnouchi, A. B. Anderson, *J. Phys. Chem. C*, **2009**, *113*, 17484.

[60] L. C. Anderson, C. E. Mooney, J. H. Lunsford, *Chem. Phys. Lett.* **1992**, *196*, 445.

[61] S. J. Teichner, *Appl. Catal*. **1990**, *62*, 1.

[62] W. A. Rigdon, X. Huang, *J. Power Sources,* **2014**, *272*, 845.

[63] C.-C. Ting, C.-H. Liu, C.-Y. Tai, S.-C. Hsu, C.-S. Chao, F.-M. Pan, *J. Power Sources*, **2015**, *280*, 166.

[64] J. Zhang, M. B. Vukmirovic, Y. Xu, M. Mavrikakis, R. R. Adzic, *Angew. Chem. Int. Ed*. **2005**, *44*, 2132.

[65] K. Sasaki, L. Zhang, R. R. Adzic, *Phys.Chem.Chem. Phys*. **2008**, *10*, 159.

[66] S. W. Sweeney, G. Roseman, C. P. Deming, N. Wang, T. A. Nguyen, *Int. J. Hydrog. Energy* **2016**, *41*, 18005.

[67] K. Liu, Y. Song, S. Chen, *Nanoscale* **2015**, *7*, 1224.

[68] K. E. Swider, C. I. Merzbacher, P. L. Hagans, D. R. Rolison, *Chem. Mater*. **1997**, *9*, 1248.

[69] E. Christoffersen, P. Liu, A. Ruban, H. L. Skriver, J. K. Norskov, *J. Catalysis* **2001**, *199*, 123.

[70] R. Kou, Y. Shao, D. Mei, Z. Nie, D. Wang, C. Wang, V. V. Viswanathan, S. Park, I. A. Aksay, Y. Lin Y. Wang, J. Lin, *J. Am. Chem. Soc*. **2011**, *133*, 2541.

[71] B. K. Min, W. T. Wallace, D. W. Goodman, *Surf. Sci. Lett.* **2006**, *600*, L7.

[72] O. Kasian, T. Luk'yanenko, A. Velichenko, R. Amadelli, *Int. J. Electrochem. Sci*. **2012**, *7*, 7915.

[73] O. I. Kasian, T. V. Luk'yanenko, P. Demchenko, R. E. Gladyshevskii, R. Amadelli, A. B. Velichenko, *Electrochim. Acta* **2013**, *109*, 63.

[74] X. Hong, Y. Sun, T. Zhu, Z. Liu, *Catalysts*, **2017**, *22*, 351.

[75] N. Lopez, T. V. W. Janssens, B. S. Clausen, Y. Xu, M. Mavrikakis, T. Bligaard, J. K. Norskov, *J. Catalysis*, **2004**, *223*, 232.

[76] Z. Awaludin, T. Okajima, T. Ohsaka, *J. Power Sources*, **2014**, *268*, 728.

[77] Z. Awaludin, M. Safuan, T. Okajima, T. Ohsaka, *J. Mater. Chem*. A, **2015**, *3*, 16791.

[78] J. C. Davies, B. E. Hayden, D. J. Pegg, M. E. Rendall, *Surf. Sci*., **2002**, *496*, 110.

[79] X. Deng, H. Tüysüz, *ACS Catalysis*, **2014**, *4*, 3701.